AJR FOCUS ON:

Hip Anatomic Variants That May Mimic Pathologic Entities on MRI: Nonlabral Variants

Mike S. Nguyen[1]
Valeriy Kheyfits[1]
Brian D. Giordano[2]
Gregory Dieudonne[1]
Johnny U. V. Monu[1]

OBJECTIVE. The hip has several anatomic variants that may be mistaken for pathologic abnormalities. The radiologist needs to be able to distinguish these variants from true abnormalities. In this review, we present nonlabral variants of the hip that can be seen on MRI.

CONCLUSION. The hip has multiple anatomic variants that may mimic disease on hip MRI. Like labral variants, nonlabral variants can be confused for true abnormalities.

In addition to labral variants, the radiologist should be aware of nonlabral variants that may mimic pathologic abnormalities on hip MRI to distinguish them from true abnormalities. These variants include synovial herniation pits, os acetabuli, iliopsoas bursa, accessory iliacus tendon, ligamentum teres, plicae, pectinofoveal fold, supraacetabular fossa, stellate crease, and tubular tracking.

Synovial Herniation Pits

Synovial herniation pits, also known as Pitt pits, appear radiographically as round radiolucencies surrounded by thin sclerotic margins and are predominantly found at the superior portion of the proximal anterior femoral neck (Fig. 1). Other cystic lesions can mimic herniation pits, including focal osteoporosis, degenerative changes, and trabecular restructuring at the anterior femoral neck. Herniation pits can be distinguished because of their characteristic subchondral or subcortical location, completely surrounding sclerosis, clear demarcation, and round-to-oval shape on MDCT [1].

Because herniation pits are found in 33% of patients with femoroacetabular impingement, whereas only 4–12% of the general population has herniation pits, Leunig et al. [2] and Panzer et al. [3] proposed a direct relationship between herniation pits and femoroacetabular impingement [2–4]. The mechanism is thought to be due to extreme hip flexion with internal rotation. This would lead to repetitive impingement on the femoral neck by the anterosuperior acetabulum, resulting in herniation of fluid into the cortical bone. An alternative proposal is an extensor mechanism caused by pressure of the iliopsoas muscle on the joint capsule with the hip in extension [2]. Activities such as running and, in particular, hurdling cause exacerbation. The presence of herniation pits should prompt assessment for the presence of femoroacetabular impingement because it is a major cause of early "primary" osteoarthritis of the hip [5].

Os Acetabuli

The acetabulum is formed from the fusion of multiple primary and accessory ossification centers that can appear as early as age 6 years [6, 7]. By ages 18–20 years, these ossification centers should have united to form one bone. However, in 2–3% of asymptomatic patients, an accessory ossification center may persist as an ossicle that is known as an os acetabulum and is typically located along the acetabular rim [8] (Fig. 2). Os acetabuli are unfused to the acetabulum and are surrounded by intact hyaline cartilage.

In addition to the nonunion of secondary acetabular ossification centers, os acetabuli can develop from incomplete healing of acetabular rim fractures and ossifications within the acetabular labrum [9]. Acquired acetabular ossifications have been described with trauma, rickets, osteomyelitis, tuberculosis, and osteochondritis dissecans [6]. Acetabular rim fragments that are difficult to differentiate from os acetabuli can also be seen in femoroacetabular impingement syndrome, which results from repetitive trauma to the acetabular rim from the femoral neck [10, 11]. Although most os acetabuli are small and asymptomatic, some os acetabuli are large enough to contribute to both acetabular rim impingement and joint stability.

Keywords: anatomic, hip, MRI, pathology, variant

DOI:10.2214/AJR.12.9861

Received August 31, 2012; accepted after revision December 16, 2012.

[1]Department of Imaging Sciences, University of Rochester Medical Center, 601 Elmwood Ave, Box 648, Rochester, NY 14642. Address correspondence to V. Kheyfits (valeriy_kheyfits@urmc.rochester.edu).

[2]Department of Orthopaedics, Division of Sports Medicine, University of Rochester Medical Center, Rochester, NY.

CME/SAM
This article is available for CME/SAM credit.

WEB
This is a web exclusive article.

AJR 2013; 201:W401–W408

0361–803X/13/2013–W401

Iliopsoas Bursa

The iliopsoas bursa is located beneath the musculotendinous portion of the iliopsoas muscle, anterior to the hip joint capsule, and lateral to the femoral vessels. The bursa separates the iliopsoas tendon from the articular capsule of the hip joint. The iliopsoas bursa is not only the largest bursa around the hip joint but also the largest bursa in the body.

In most patients, the iliopsoas bursa is normally collapsed and not seen on MRI. In 15% of asymptomatic patients, the iliopsoas bursa directly communicates with the hip joint because there is a congenital connection between the hip joint and the iliopsoas bursa [12]. This is seen as the bursa being distended by a small amount of synovial fluid or intraarticular contrast material (Fig. 3). However, this direct communication may also be acquired if there is a tear in the joint capsule due to chronic friction from the iliopsoas tendon. This would allow the joint fluid to enter into and distend the bursa [13]. Other acquired inflammatory or mechanical conditions include trauma, osteoarthritis, avascular necrosis, rheumatoid arthritis, synovial chondromatosis, pigmented villonodular synovitis, gout, and pyogenic infection [12].

Accessory Iliacus Tendon

The iliopsoas tendon complex includes the iliopsoas tendon, which attaches to the lesser trochanter, the lateral portion of the iliacus muscle that attaches directly to the anterior portion of the proximal femoral diaphysis, and the accessory iliacus tendon, which is a thin intramuscular tendon within the lateral portion of the iliacus muscle [14]. The accessory iliacus tendon is very common and is found in 66% of patients on MR arthrograms [15]. Although the accessory iliacus tendon is usually asymptomatic, in one anatomic study [16], three examples of a slipped accessory tendon piercing the femoral nerve were described. Separating the accessory iliacus tendon from the iliopsoas tendon is a thin plane of fatty fascia that is seen as high signal intensity on T1-weighted imaging (Fig. 4). Although it can mimic a longitudinal tear of the iliopsoas tendon, the accessory iliacus tendon can be differentiated from a tear by fat-suppression sequences.

Ligamentum Teres

Arising from the transverse acetabular ligament along the inferior margin of the acetabulum, the ligamentum teres is attached to the periosteum by two bands located along the ischial and pubic margins of the acetabular notch. It is an important hip stabilizer, especially during adduction, flexion, and external rotation. The ligamentum teres has a smooth contour and is a relatively homogeneous structure. It has a cordlike appearance with mild expansion at its insertion on the femoral head. On MRI, the ligamentum teres is hypointense on all pulse sequences; however, areas of slightly increased signal intensity may be seen near its attachment to the fovea capitis femoris [17]. In patients with developmental dysplasia of the hip, the ligamentum teres may be thickened, hypertrophied, or elongated. Some patients may have congenital absence of the ligamentum teres [8].

Plicae

Plicae are synovial folds commonly located at the interface of articular surfaces, and they represent embryonic remnants. In addition to synovial fluid production, plicae also contain neurovascular structures and stabilize the joint.

In an anatomic study, Fu et al. [18] characterized the hip plicae by form (flat or villous) and location (labral, neck, and ligamental). The labral plica is adjacent to the inferomedial region of the acetabular labrum, the neck plica is in the synovial reflection at the superior portion of the femoral neck, and the ligamental plica is at the acetabular base of the ligament of the head of the femur (Fig. 5). On MR arthrography, the labral, neck, and ligamental plicae are found in 76%, 97%, and 78%, respectively, of asymptomatic hips.

Plicae normally slip between the articular surfaces and generally are asymptomatic. However, they can become symptomatic by either mechanical impingement or mass effect on other structures. Four cases of symptomatic hip plicae have been reported in the literature [19–21]. Symptoms include progressive pain with activity, audible click, or effusion. Of the three locations, the labral plica is most likely to be symptomatic because it can become entrapped by either the acetabular labrum or the transverse ligament, both of which are located parallel to the plica [8]. The neck or ligamentous plica is unlikely to be symptomatic because it does not become entrapped. There is no significant association between the labral, neck, and ligamental plicae and labral tears, femoroacetabular impingement, and osteoarthritis [22].

Pectinofoveal Fold

The pectinofoveal fold, also known as the middle retinaculum of Weitbrecht, extends from the lesser trochanter to the fovea capitis and contains the posteroinferior retinacular arteries and branches of the medial femoral circumflex artery. The pectinofoveal fold was originally described as a plica, but unlike plicae, the pectinofoveal fold is unlikely to become symptomatic [8, 23].

The pectinofoveal fold is very common and can be found in 95% of cases on hip MR arthrography and in 99% of cases on arthroscopy [23] (Figs. 6 and 7). The fold can have various appearances and attachment sites. The joint capsule is a more common insertion site (75% of cases) than the femur (25% of cases). Location is the most important criterion to confidently identify the pectinofoveal fold; if the structure is found elsewhere in the joint, it should be considered a plica. A smooth contour is slightly more common (52% of cases) than an irregular one (48% of cases). Thus, an irregular-appearing fold should not necessarily be considered abnormal or pathologic.

Supraacetabular Fossa

The supraacetabular fossa is characteristically located at the 12 o'clock position of the acetabular roof on both coronal and sagittal imaging (Fig. 8). For MR arthrography, Dietrich et al. [24] classified supraacetabular fossa into two types: type 1 was filled with contrast material on MR arthrograms and type 2 was filled with cartilage. On MR arthrography, types 1 and 2 are found in 1.6% and 8.9% of cases, respectively. Although it can mimic an acetabular cartilage defect [25], supraacetabular fossa can be easily distinguished from a defect by location, the presence of normal underlying marrow signal intensity on MRI, and the absence of cartilage defects on arthroscopy.

Stellate Crease (Stellate Lesion)

The stellate crease, also known as stellate lesion, represents a bare area within the acetabular articular surface deficient of hyaline cartilage. It is located above the anterosuperior margin of the acetabulum and medial to the supraacetabular fossa [8] (Fig. 9). On arthroscopy, the stellate crease appears as a focal area of hyaline cartilage deficiency in the acetabular roof. On MRI, the stellate crease can appear as a focal area of cartilage deficiency in the acetabular roof and can be mistaken for a focus of chondromalacia or osteochondral defect. Although the supraacetabular fossa is always found at the 12 o'clock location on MRI, the stellate crease is always medial to this location. The stellate crease can be further distinguished from the supraacetabular fossa because the stellate crease is in continuity with the acetabular notch but not with the supraacetabular fossa [24]. The acetabular notch is a

depression at the anteroinferior margin of the acetabulum that forms the acetabular foramen when it is bridged by the transverse ligament. The stellate crease, which is frequently found in the young adult, should also be differentiated from the triradiate cartilage, which is present only in the immature skeleton [8, 26].

Tubular Tracking of Contrast on MR Arthrography

Lien et al. [27] were the first to describe tubular intraosseous tracking of contrast in the acetabular fossa during MR arthrography. Tubular tracking was observed in 16% of asymptomatic hips. The tracking consistently originated from the posterior margin of the acetabular fossa. Several causes of tubular tracking have been proposed, including degeneration-associated cysts and intraosseous ganglia; the most probable cause is repeated pumping of joint fluid through the nutrient foramina of the acetabular fossa. Because the superior portion of the acetabular fossa is void of synovial lining, the acetabular branches of obturator vessels can branch into the nutrient foramina that are located at the margins of the acetabular fossa [25]. Lien et al. surmised that repeated pumping of joint fluid through the nutrient foramina causes dilatation and gives tubular tracking its characteristic appearance.

If the tubular tracks become prominent, they can be easily visualized by other modalities, such as radiography, CT, and non-MRI arthrography. They will appear as linear blind-ending structures that originate from the margins of the acetabular fossa. On CT, tracks appear as tubular structures with thin sclerotic borders without periostitis or cortical changes (Fig. 10). On fluid-sensitive MRI sequences, the tracks have signal-intensity characteristics consistent with fluid or contrast (Fig. 11). Furthermore, the marrow surrounding the tracks should show normal signal intensity. In an appropriate setting, the lesion may be mistaken for an atypical presentation of osteoid osteoma.

In summary, the hip has several anatomic variations that may be mistaken for pathologic entities on MRI. Like labral variants, nonlabral anatomic variants can be confused for abnormalities. Awareness of these anatomic variants will reduce unnecessary workup, patient anxiety, and overtreatment.

References

1. Panzer S, Esch U, Abdulazim AN, Augat P. Herniation pits and cystic-appearing lesions at the anterior femoral neck: an anatomical study by MSCT and microCT. *Skeletal Radiol* 2010; 39:645–654
2. Leunig M, Beck M, Kalhor M, Kim YJ, Werlen S, Ganz R. Fibrocystic changes at anterosuperior femoral neck: prevalence in hips with femoroacetabular impingement. *Radiology* 2005; 236:237–246
3. Panzer S, Augat P, Esch U. CT assessment of herniation pits: prevalence, characteristics, and potential association with morphological predictors of femoroacetabular impingement. *Eur Radiol* 2008; 18:1869–1875
4. Leunig M, Mast NH, Impellizerri FM, Ganz R, Panaro C. Arthroscopic appearance and treatment of impingement cysts at femoral head-neck junction. *Arthroscopy* 2012; 28:66–73
5. Tannast M, Siebenrock KA, Anderson SE. Femoroacetabular impingement: radiographic diagnosis—what the radiologist should know. *AJR* 2007; 188:1540–1552
6. Klaue K, Durnin CW, Ganz R. The acetabular rim syndrome: a clinical presentation of dysplasia of the hip. *J Bone Joint Surg Br* 1991; 73:423–429
7. Ponseti IV. Growth and development of the acetabulum in the normal child: anatomical, histological, and roentgenographic studies. *J Bone Joint Surg Am* 1978; 60:575–585
8. DuBois DF, Omar IM. MR imaging of the hip: normal anatomic variants and imaging pitfalls. *Magn Reson Imaging Clin N Am* 2010; 18:663–674
9. Hergan K, Oser W, Moriggl B. Acetabular ossicles: normal variant or disease entity? *Eur Radiol* 2000; 10:624–628
10. Kassarjian A, Yoon LS, Belzile E, Connolly SA, Millis MB, Palmer WE. Triad of MR arthrographic findings in patients with cam-type femoroacetabular impingement. *Radiology* 2005; 236:588–592
11. Martinez AE, Li SM, Ganz R, Beck M. Os acetabuli in femoro-acetabular impingement: stress fracture or unfused secondary ossification centre of the acetabular rim? *Hip Int* 2006; 16:281–286
12. Varma DG, Richli WR, Charnsangavej C, Samuels BI, Kim EE, Wallace S. MR appearance of the distended iliopsoas bursa. *AJR* 1991; 156:1025–1028
13. Bianchi S, Martinoli C, Keller A, Bianchi-Zamorani MP. Giant iliopsoas bursitis: sonographic findings with magnetic resonance correlations. *J Clin Ultrasound* 2002; 30:437–441
14. Polster JM, Elgabaly M, Lee H, Klika A, Drake R, Barsoum W. MRI and gross anatomy of the iliopsoas tendon complex. *Skeletal Radiol* 2008; 37:55–58
15. Tatu L, Parratte B, Vuillier F, Diop M, Monnier G. Descriptive anatomy of the femoral portion of the iliopsoas muscle: anatomical basis of anterior snapping of the hip. *Surg Radiol Anat* 2001; 23:371–374
16. Spratt JD, Logan BM, Abrahams PH. Variant slips of psoas and iliacus muscles, with splitting of the femoral nerve. *Clin Anat* 1996; 9:401–404
17. Cerezal L, Kassarjian A, Canga A, et al. Anatomy, biomechanics, imaging, and management of ligamentum teres injuries. *RadioGraphics* 2010; 30:1637–1651
18. Fu Z, Peng M, Peng Q. Anatomical study of the synovial plicae of the hip joint. *Clin Anat* 1997; 10:235–238
19. Atlihan D, Jones DC, Guanche CA. Arthroscopic treatment of a symptomatic hip plica. *Clin Orthop Relat Res* 2003; 411:174–177
20. Frich LH, Lauritzen J, Juhl M. Arthroscopy in diagnosis and treatment of hip disorders. *Orthopedics* 1989; 12:389–392
21. Hélénon C, Bergevin H, Aubert JD, Lebreton C, Hélénon O. Plication of the hip synovium above the femur neck (in French). *J Radiol* 1986; 67:737–740
22 Bencardino JT, Kassarjian A, Vieira RL, Schwartz R, Mellado JM, Kocher M. Synovial plicae of the hip: evaluation using MR arthrography in patients with hip pain. *Skeletal Radiol* 2011; 40:415–421
23. Blankenbaker DG, Davis KW, De Smet AA, Keene JS. MRI appearance of the pectinofoveal fold. *AJR* 2009; 192:93–95
24. Dietrich TJ, Suter A, Pfirrmann CW, Dora C, Fucentese SF, Zanetti M. Supraacetabular fossa (pseudodefect of acetabular cartilage): frequency at MR arthrography and comparison of findings at MR arthrography and arthroscopy. *Radiology* 2012; 263:484–491
25. Keene GS, Villar RN. Arthroscopic anatomy of the hip: an in vivo study. *Arthroscopy* 1994; 10:392–399
26. Stoller DW. *Magnetic resonance imaging in orthopaedics and sports medicine*, 3rd ed. Philadelphia, PA: Lippincott Williams & Wilkins, 2006
27. Lien LC, Hunter JC, Chan YS. Tubular acetabular intraosseous contrast tracking in MR arthrography of the hip: prevalence, clinical significance, and mechanisms of development. *AJR* 2006; 187:807–810

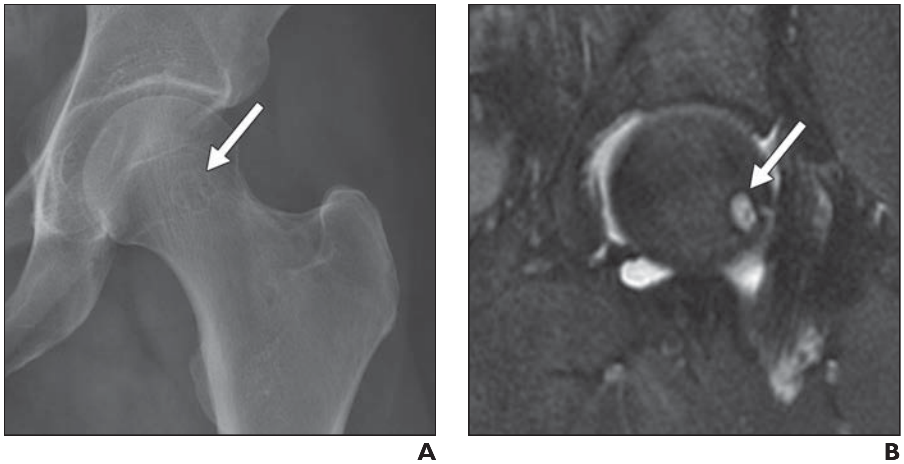

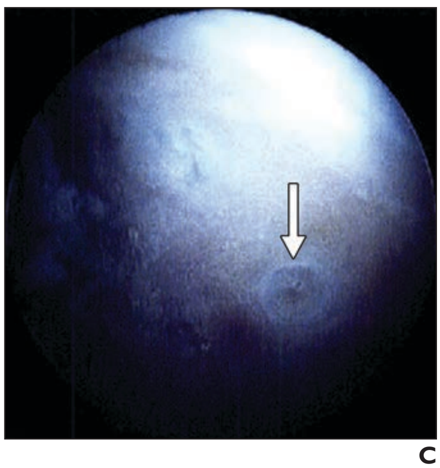

Fig. 1—40-year-old woman with synovial herniation pits.
A, On radiograph, herniation pits (*arrow*) appear as lucent lesions with thin sclerotic rims at anterior femoral head–neck junction.
B, On coronal fat-saturated intermediate-weighted MRI, herniation pits (*arrow*) are hyperintense to skeletal muscle on T2-weighted images and may approach fluid intensity. Marrow edema may occasionally be seen.
C, On arthroscopy, herniation pits (*arrow*) appear as well-defined cortical defects. There is increased association of synovial herniation pits and femoroacetabular impingement syndrome.

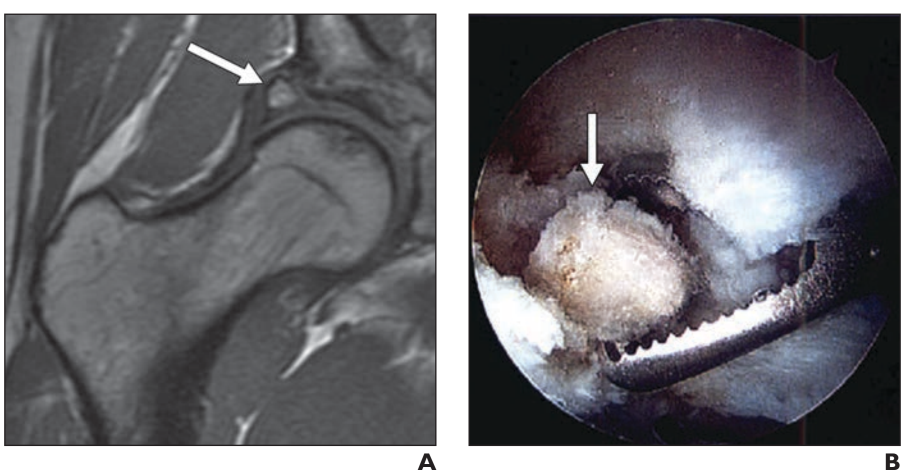

Fig. 2—Os acetabuli in two different patients.
A and **B,** 30-year-old man. Coronal T1-weighted MRI (**A**) and arthroscopic image (**B**) show os acetabulum (*arrows*). Os acetabuli can be congenital or acquired. Acetabular rim fragments from femoroacetabular impingement syndrome can be difficult to differentiate from os acetabuli.

(Fig. 2 continues on next page)

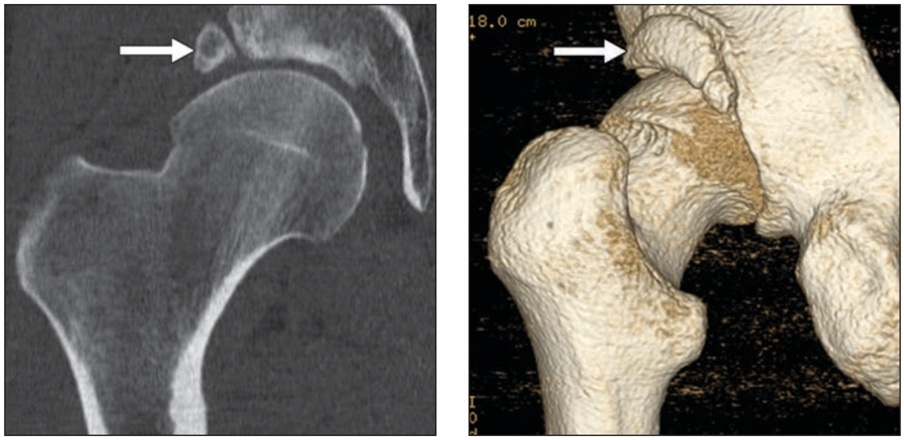

C D

Fig. 2 (continued)—Os acetabuli in two different patients.
C and **D,** 26-year-old man. Coronal (**C**) and volume-rendered (**D**) CT images show large os acetabulum (*arrows*). If it is large enough, os acetabulum can contribute to both acetabular rim impingement and joint stability.

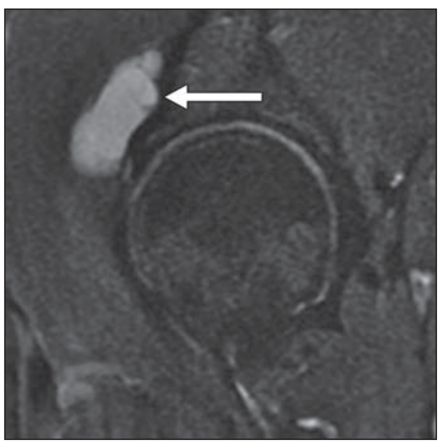

Fig. 3—26-year-old man with iliopsoas bursa. Sagittal fat-saturated intermediate-weighted image shows iliopsoas bursa (*arrow*). Iliopsoas bursa is normally collapsed and not seen on MRI. In 15% of asymptomatic patients, there is direct congenital communication between hip joint and iliopsoas bursa. Direct communication can also be acquired from various inflammatory or mechanical conditions.

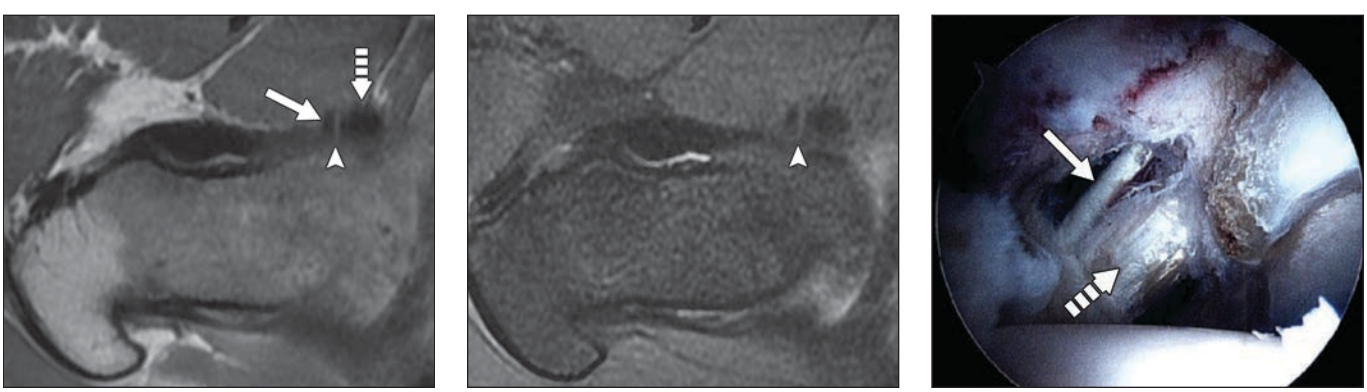

A B C

Fig. 4—Two different patients with accessory iliacus tendon.
A and **B,** 16-year-old boy. Axial proton density–weighted (**A**) and axial fat-saturated intermediate-weighted (**B**) images show that plane of fatty fascia (*arrowheads*, **A** and **B**) separates accessory iliacus tendon (*solid arrow*, **A**) from iliopsoas tendon (*dotted arrow*, **A**). This fat plane can be differentiated from longitudinal tear of iliopsoas tendon by suppressing fat signal with fat saturation techniques.
C, 32-year-old woman. Arthroscopic image shows accessory iliacus tendon (*solid arrow*) and iliopsoas tendon (*dotted arrow*).

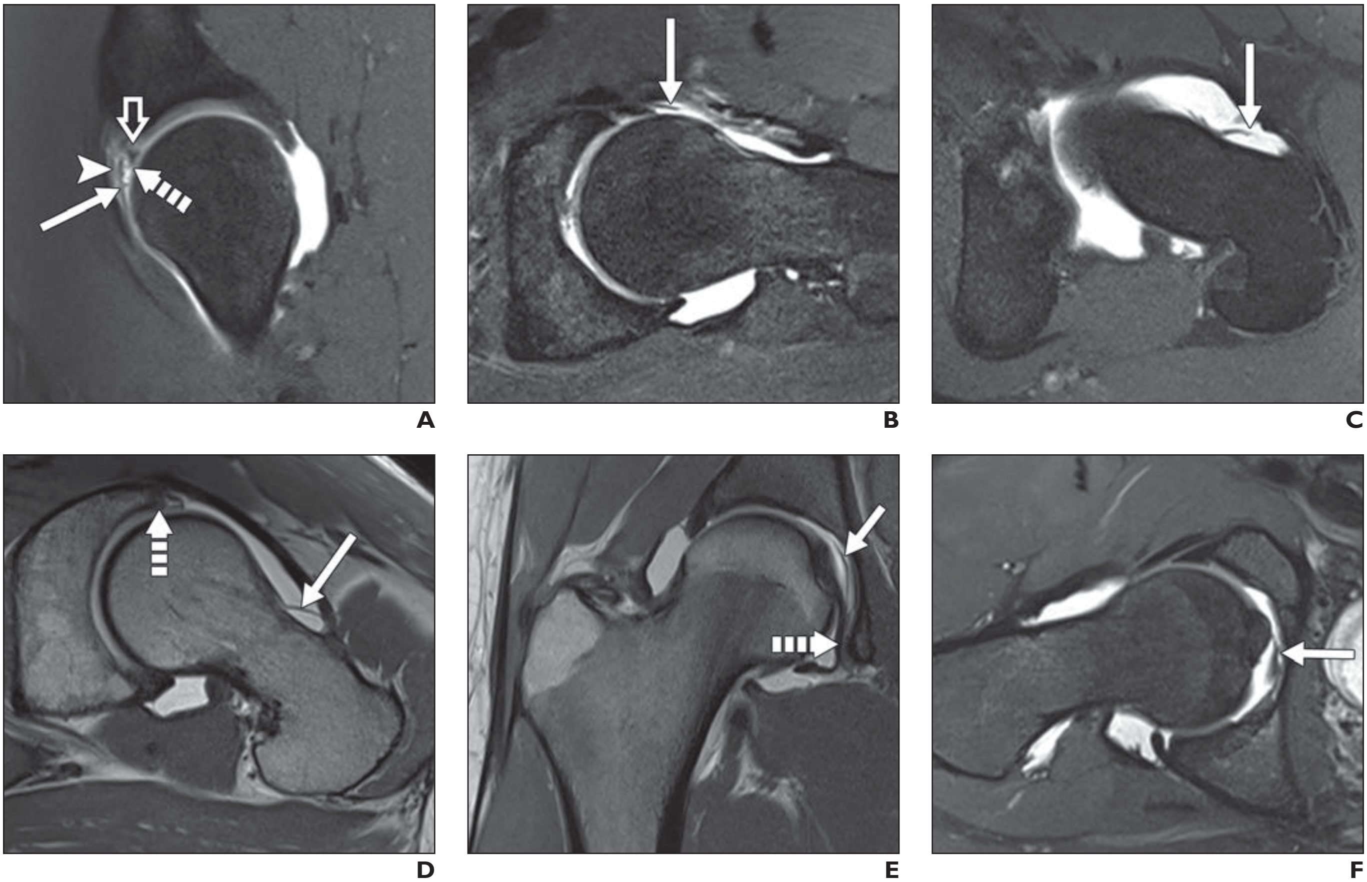

Fig. 5—Plicae in three different patients.
A and **B,** 17-year-old boy. Sagittal T1-weighted (**A**) and axial oblique fat-saturated intermediate-weighted (**B**) MR arthrographic images show labral plica (*solid arrows*, **A** and **B**) as hypointense linear structure interposed between anterosuperior labrum (*dotted arrow*, **A**) and anterior joint capsule (*arrowhead*, **A**). Anterior labral tear (*open arrow*, **A**) is incidentally noted.
C and **D,** 30-year-old man. Axial fat-saturated T1-weighted (**C**) and axial oblique proton density–weighted (**D**) MR arthrographic images show neck plica (*solid arrows*, **C** and **D**). Anterior superior labral tear (*dotted arrow*, **D**) is incidentally noted.
E and **F,** 18-year-old woman. Coronal proton density–weighted (**E**) and axial oblique fat-saturated intermediate-weighted (**F**) MR arthrographic images show ligamental plica (*solid arrows*, **E** and **F**). Ligamental plica is shown paralleling ligamentum teres (*dotted arrow*, **E**).

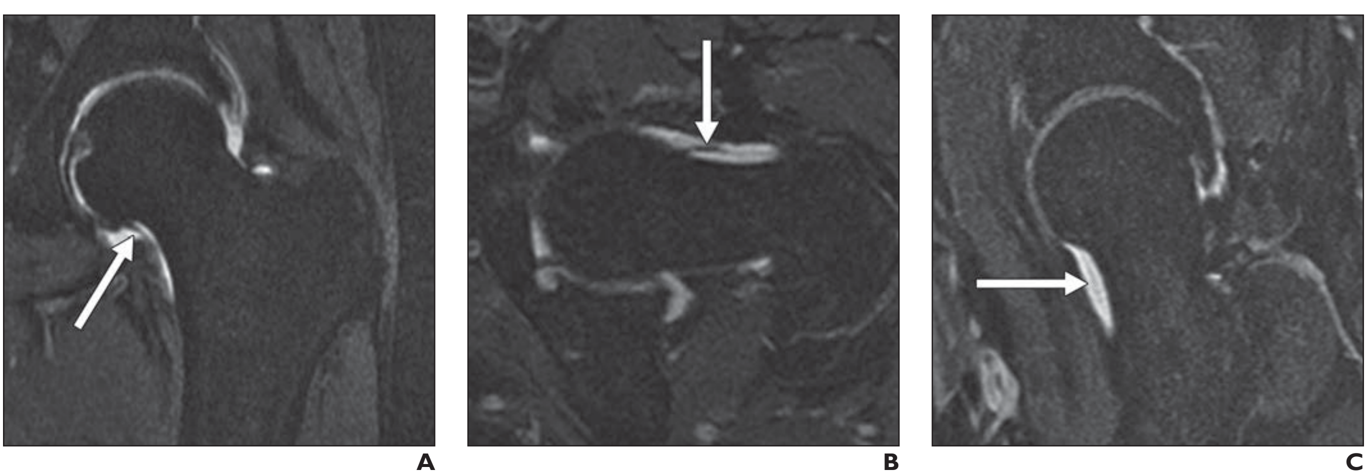

Fig. 6—60-year-old woman with pectinofoveal fold.
A–C, Pectinofoveal fold (*arrows*) is seen as hypointense linear structure in multiple planes on coronal (**A**), axial (**B**), and sagittal (**C**) fat-saturated intermediate-weighted images. Pectinofoveal fold is very common and can be found in 95% of cases on hip MR arthrography and in 99% of cases on arthroscopy. Location is most important criterion to differentiate pectinofoveal fold from plica. Both smooth and irregular contours can normally be found.

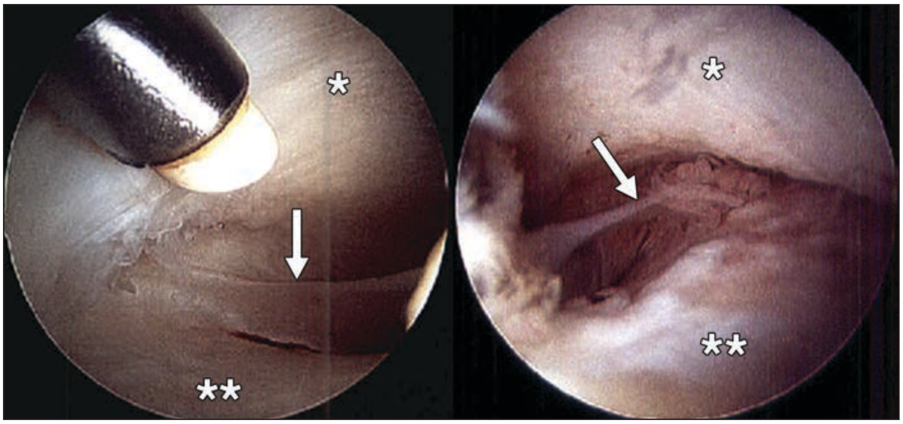

Fig. 7—30-year-old man with pectinofoveal fold. Two arthroscopic images show pectinofoveal fold (*arrows*) in relation to acetabulum (*single asterisks*) and femoral head (*double asterisks*).

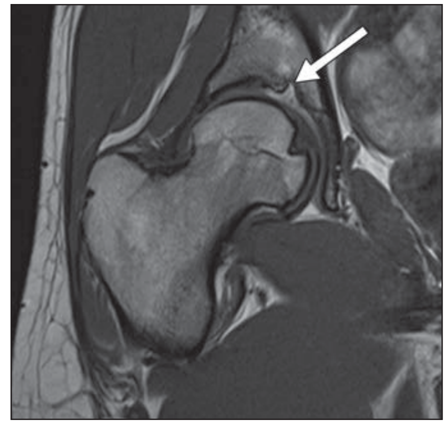

Fig. 8—15-year-old girl with supraacetabular fossa. Supraacetabular fossa (*arrow*) is characteristically located at 12 o'clock position of acetabular roof, as shown in this coronal proton density–weighted image. Supraacetabular fossa can be distinguished from cartilage defect by location, presence of normal marrow signal intensity on MRI, and absence of cartilage defects on arthroscopy.

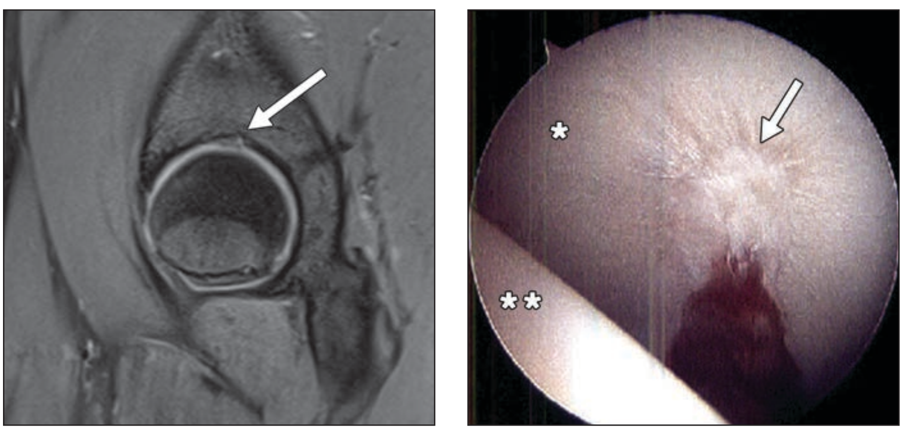

A **B**

Fig. 9—15-year-old girl with stellate crease (same patient as in Fig. 8).
A and **B,** On sagittal fat-saturated proton density–weighted (**A**) and arthroscopic (**B**) images, stellate crease (*arrows*, **A** and **B**) is seen as shallow puckering and deficiency in articular cartilage of acetabulum. Relationship of stellate crease with acetabulum (*single asterisk*, **B**) and femoral head (*double asterisks*, **B**) is shown. Although supraacetabular fossa is always found at 12 o'clock location on MRI, stellate crease is always medial to this location. Stellate crease can be further distinguished from supraacetabular fossa because stellate crease is in continuity with acetabular notch but not with supraacetabular fossa.

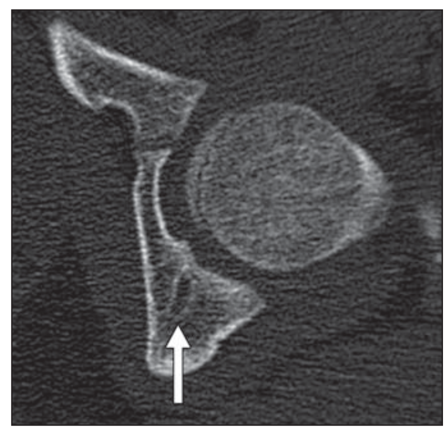

Fig. 10—11-year-old boy with tubular tracking. Axial CT image in bone window shows characteristic appearance of tubular structure (*arrow*) with thin sclerotic borders without periostitis or cortical changes.

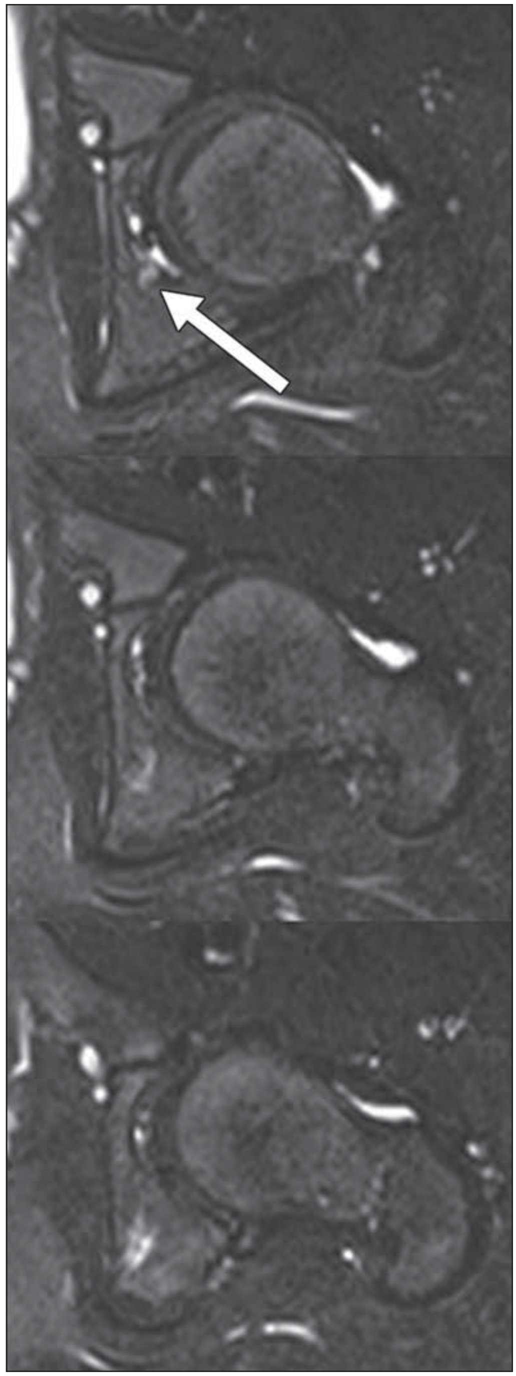

Fig. 11—11-year-old boy with tubular tracking (same patient as in Fig. 10). Serial axial fat-saturated intermediate-weighted images show that tubular tracks (*arrow*) are blind-ending tubular structures filled with fluid.